IEEE Access
Multidisciplinary ⋮ Rapid Review ⋮ Open Access Journal

Received 21 November 2022, accepted 30 November 2022, date of publication 2 December 2022, date of current version 9 December 2022.

Digital Object Identifier 10.1109/ACCESS.2022.3226514

RESEARCH ARTICLE

Thermal Wave Variation Anticipation Under Minute Scale Time-Advance With Low-Pass NGD Digital Circuit

BLAISE RAVELO[1], (Member, IEEE), MATHIEU GUERIN[2,3], (Member, IEEE), JAROSLAV FRNDA[4,5], (Senior Member, IEEE), LALA RAJAOARISOA[6], (Member, IEEE), AND WENCESLAS RAHAJANDRAIBE[2,3], (Member, IEEE)

[1]School of Electronic and Information Engineering, Nanjing University of Information Science and Technology, Nanjing, Jiangsu 210044, China
[2]CNRS, Aix-Marseille University, 13007 Marseille, France
[3]IM2NP (UMR7334), University of Toulon, 83130 La Garde, France
[4]Department of Quantitative Methods and Economic Informatics, Faculty of Operation and Economics of Transport and Communication, University of Zilina, 01026 Zilina, Slovakia
[5]Department of Telecommunications, Faculty of Electrical Engineering and Computer Science, VSB–Technical University of Ostrava, 70800 Ostrava, Czech Republic
[6]Centre for Digital Systems, IMT Nord Europe, University of Lille, 59000 Lille, France

Corresponding author: Mathieu Guerin (mathieu.guerin@im2np.fr)

This work was supported in part by Fonds d'Intervention Recherche, Aix-Marseille University (FIR 2022 AMU) Invited Professor Program, in part by SATIE National Agency, in part by the Ministry of Education of the Czech Republic under Project SP2022/5, and in part by the Slovak Grant Agency for Science [Vedecká grantová agentúra (VEGA)] under Grant 1/0157/21.

ABSTRACT Over the emerging industry 4.0 era, the building control system performance depends on the development of smart sensor technology. Nowadays, the building control engineers challenge on the design of high-capacity smart sensor susceptible to operate with high speed of data processing. In this context, this paper introduces a pioneer research work on the negative group delay (NGD) circuit original application for room temperature anticipation useful for smart-building control. The real-time anticipation of sensor data by using a low-pass (LP) NGD digital circuit is studied. This approach enables minimizing the latency time for optimizing control action. The unfamiliar LP-NGD digital circuit design method and theoretical formulation are described for anticipating thermal wave experimentation in real-time. The digital circuit equation coefficients are computed regarding the time-advance of anticipated thermal completely arbitrary waveform signal. The main interest of using the NGD method-based for thermal wave anticipation regarding temperature variation from heater and freezer control is demonstrated. The anticipation feasibility is illustrated from the minute scale time-advance LP-NGD digital circuit implemented on the STM32® microcontroller unit. The NGD characterization is performed from frequency domain analysis and cosine waveform pulse transient test. Then, the -30 seconds to -10 seconds real-time-advance of temperature variation is verified by calculation and experimentation. The present study result opens a promising NGD method application for the advanced fault control of a future industrial system by anticipating system failures.

INDEX TERMS Group delay (NGD), low-pass (LP) NGD, experimental study, NGD digital circuit, NGD design, NGD analysis method, thermal wave, real-time anticipation, time-advance, NGD application.

I. INTRODUCTION

Environmental temperature control plays a central role in the future development of civilian society and industrial system improvement. In this context, several researchers elaborated different approaches to building performance improvements by means of temperature control.

A. CHALLENGE ON DELAY EFFECT FOR CONTROLLED BUILDING PERFORMANCES

So far, tremendous effort is deployed for smart-city design by overcoming the challenge of smart-building

The associate editor coordinating the review of this manuscript and approving it for publication was Yiqi Liu.

control [1], [2], [3], [4]. For instance, Thavlov and Bindner in [2] and Rajaoarisoa et al. in [3] proposed an intelligent heating system to optimize energy consumption and habitant comfort. Furthermore, several building thermal models were developed during the design stage for even better control of habitant comfort [4], [5], [6]. Then, one of today's research challenges for thermal building research engineers is the prediction of physical parameters of the environment as temperature [7]. Like an industrial system, the effectiveness of the smart-building control depends systematically on the sensor and operating signal delay performances. As presented in [8] and [9], one can deploy different generations of industrial wireless sensors for future system control techniques assessment. An overview of some recent advanced technologies and open problems of time-delay systems is reviewed in [10]. Despite the progress of the smart factory and industry 4.0 concept, there are different open-questions related to the undesirable effects of time delay on system control and robustness [11], [12]. Some criteria for system delay-dependence were evoked to preserve industrial system performances [13], [14]. Communication delays constitute a major limiting factor for the development of the industrial system remote control.

To face up such delay problems, an unconventional and original solution consisting of exploring the electronic circuit presenting unfamiliar negative group delay (NGD) property is developed in the present study.

B. STATE OF THE ART ON NGD CIRCUIT

Some visionary research works [15], [16], [17], [18] state that the NGD circuit can be applied to reduce or even cancel out signal delay. But so far, NGD circuit engineering is not developed enough due to the misunderstanding of its fundamental characteristics and lack of industrial applications. However, from different experiments, it was demonstrated with different electronic circuit topologies that the NGD circuits can allow propagation of output signals in time-advance compared to their input ones [19], [20], [21], [22], [23], [24]. But the NGD method seems a victim of its counterintuitive effect on the natural delay perception. To highlight the possibility and feasibility of experimenting with an NGD circuit, it is worth to notice that NGD does not contradict the notion of causality as shown in [19] and [20]. When dealing with NGD circuit engineering, many questions come naturally about the meaning of this counterintuitive effect. For better interpretation and analysis, a fundamental theory of NGD function was initiated by analogy with the filter [25], and different topologies were classified. From this original NGD circuit theory, some simple topologies have been identified to behave as:

- Low-pass (LP) type NGD topologies [15], [16], [17], [18], [19], [20], [21], [22], [23], [24], [25], [26], [27], [28] which are specified by their group delay (GD) diagram presenting negative value at very low frequencies (VLFs) or quasi-static,
- Bandpass (BP) type topologies [29], [30] because their GD is negative in certain frequency bands delimited by lower and upper specific frequencies. This type of BP-NGD topology is regularly deployed for radio frequency (RF) and communication circuits.

Nevertheless, most of the research works on NGD circuit engineering were performed with analog networks constituted by a classical resistor, R, inductor, L, and capacitor, C, lumped components [15], [16], [17], [18], [19], [20], [21], [22], [23], [24], [25], [26], [27], [28], [29], [30], [31], [32]. Because of the R, L and C manufacturing technology limitations, it was practically unfeasible to design and fabricate NGD circuits with time-advance with an absolute value of more than one second.

C. PAPER ORIGINALITY AND OUTLINE

In this paper, an innovative method to remedy this challenging limitation is proposed by designing digital NGD circuits with more than one second advance in absolute value. However, very few research works are performed on the design engineering of NGD circuits [33], [34]. An original and pioneer research work about NGD digital circuit application to solve the real-time anticipation of industrial system signals is initiated in the present paper. The unfamiliar NGD method is expected to be a promising solution to the problem of real-time remote access to industrial data [35], [36] and also the prediction of anomalies [37]. This pioneer research work is aimed to develop an original method of thermal wave signal anticipation by using a typical LP-NGD digital circuit.

The present paper is organized into five main sections as follows:

- Section II describes the test protocol of temperature measurement with a commercial sensor. The specifications of the sensor employed in this NGD study are defined. Then, the characteristics of the used commercial digital board embedding microcontroller unit (MCU) are recalled. Also, a method explaining how to implement an LP-NGD type digital circuit dedicated to sensor signal anticipation is introduced.
- Section III elaborates on the general theory and design engineering of the LP-NGD digital circuit. The canonical form of the transfer function (TF) representing the unfamiliar circuit is analytically defined. Then, the difference equation enabling to design of the digital function is described.
- Section IV explores the feasibility study of the NGD method of signal anticipation. The LP-NGD digital circuit proof-of-concept (POC) is designed. The thermal wave anticipation in real-time is presented.
- Section V is focused on the LP-NGD digital circuit design and implementation in the temperature sensing system. The LP-NGD circuit is developed by using a commercial digital board embedding MCU integrated circuit (IC). The experimental validation of thermal wave anticipation in real-time is demonstrated.
- Section VI is the conclusion of the paper.

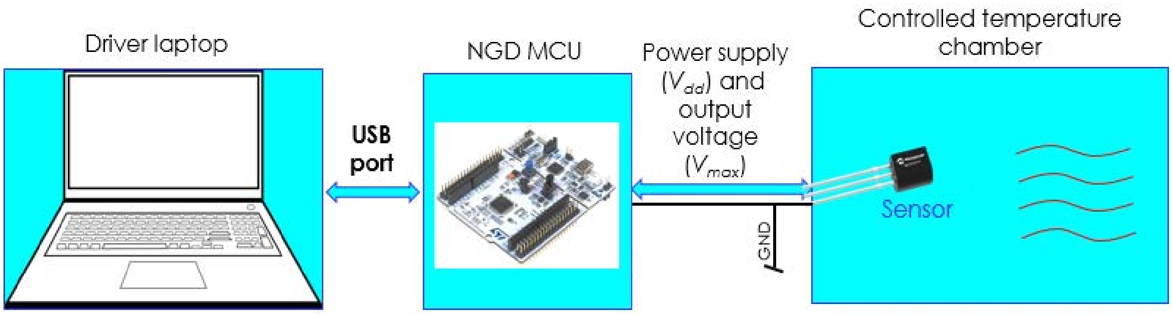

FIGURE 1. Configuration of real-time anticipated temperature test based on heated sensor configuration.

II. DESCRIPTION OF TEMPERATURE REAL-TIME MEASUREMENT TEST PROTOCOL

The present section introduces the measurement test protocol of real-time temperature variation. The synoptic of the real-time test setup is introduced. Then, the specifications of the employed test device during the unfamiliar NGD experimental study are described.

A. GENERAL SYNOPTIC OF THE TEMPERATURE VARIATION TEST SETUP

To reproduce the general configuration of temperature variation, the experimental setup is introduced in Fig. 1. It acts as challenging real-time sensing of thermal chamber temperature $T(t)$ which is time-dependently varying. It consists of the temperature sensor used to control the thermal comfort in the room. The provided thermal wave signal represents sensed environment temperature. The last one becomes the input of the LP-NGD digital circuit. Matching the output signal of the probe to the specifications of the MCU-based digital platform is particularly important to ensure data processing quality. As shown on the left of Fig. 1, the schematic shows a USB interconnection between a laptop and the MCU board. The laptop PC serves as a driver of the MCU board but also for data acquisition and storage.

B. SPECIFICATION OF THE TEMPERATURE SENSOR EMPLOYED DURING THE NGD TEST

The experimental study of the LP-NGD digital circuit application developed in this research work is based on a test protocol constituted by a commercial temperature sensor. This last one is an IC acting as a low-power linear active thermistor referenced MCP9701A-E TO which is manufactured by Microchip® [38]. The employed sensor converts ambient temperature into an analog voltage. The MCP9701A-E TO main specifications as power supply V_{dd}, and input//output dynamic ranges are indicated in Table 1. The sensor operates over a wide range of measured temperatures with accurate resolution ΔT.

The characteristic equation relating sensed real-time ambient temperature $T(t)$ (expressed in °C) and the provided equivalent voltage $v_T(t)$ (expressed in Volts) is determined by a linear relationship [38]:

$$T(t) = \frac{v_T(t) - a_0}{a_1} \tag{1}$$

where a_0 and a_1 are conversion real coefficients provided by the manufacturer.

TABLE 1. Specifications of the sensor [39] employed during the employed and unfamiliar real-time NGD digital circuit.

Description	Parameters	Values
Power supply	V_{dd}	5 V_{DC}
Measured temperature resolution	ΔT	+/-2°C
Input temperature dynamic range	T_{min}	-40°C
	T_{max}	125°C
Output voltage dynamic range	V_{min} (GND)	0 V
	V_{max}	2.8375 V
Conversion coefficients of equation (1)	a_0	0.4
	a_1	0.0195
Power supply	V_{dd}	5 V_{DC}

The sensor characteristic coefficient values provided by the manufacturer are indicated in Table 1.

In the following section, the feasibility study for the real-time anticipation of sensed temperature by means of LP-NGD circuit is explored.

Before the unfamiliar NGD investigation, the specifications of the MCU digital board will be presented in the next section.

C. SPECIFICATIONS OF THE MCU DIGITAL BOARD

The experimental investigation was performed by implementing an LP-NGD digital circuit on a commercial MCU board. It acts as the STM32® MCU board manufactured by STMicroelectronics® [39]. The digital circuit implementation platform is a Nucleo L476RG development board. The test board platform uses an STM32L476RG MCU IC package having 64-pins. The test board is fed on V_{dd} pin via the USB cable connected to the control station. The main specifications of the implementation board as microprocessor operating frequency, analog-digital-converter (ADC) and digital-analog converter (DAC) precision are addressed in Table 2.

TABLE 2. Specifications of the board [39] to implement the employed and unfamiliar NGD digital circuit.

Description	Parameters	Values
Power supply	V_{dd}	5 V_{DC}
Microprocessor operating frequency	-	80 MHz
Digital resolution	-	12 bits
Quantum resolution	ΔV	0.8 mV
Input voltage dynamic range	V_{min} (GND)	0 V
	V_{max}	3.3 V
Sampling period	T_s	187 ns

The MCU input analog voltage is limited between V_{min} and V_{max} under quantum resolution ΔV and sampling period, T_s.

The following subsection is focused on the design of the LP-NGD digital circuit.

III. THEORETICAL DESIGN APPROACH OF UNFAMILIAR LP-NGD DIGITAL CIRCUIT

The general representation of an unfamiliar LP-NGD circuit by means TF approach is defined. The basic LP-NGD specifications are expressed from frequency-domain analysis of TF magnitude and GD. The design approach of the LP-NGD POC is introduced in the present section.

A. GENERAL DEFINITION ENABLING TO ELABORATE UNFAMILIAR LP-NGD CIRCUIT

It is particularly essential to become familiar with the basic definition before starting the preliminary LP-NGD theory. By denoting s the Laplace variable, let us consider a system with symbolic input $X(s)$ and output $Y(s)$. The input and output interaction with the NGD circuit TF:

$$N(s) = \frac{Y(s)}{X(s)} \tag{2}$$

can be represented by the block diagram of Fig. 2.

The NGD cut-off frequency is chosen, to perform the circuit design, in the function of the desired time-advance $t_n < 0$ by the relationship:

$$f_n = \frac{1}{2\pi\,|t_n|}. \tag{3}$$

The associated first-order TF traditionally defined by the ratio:

$$N(s) = \frac{1 + a\,s}{1 + b\,s} \tag{4}$$

with real positive coefficients a and b. After identification, the LP-NGD TF to be explored in the empirical study can be formulated by:

$$N(s) = \frac{1 + (\sqrt{5} - 1)t_n\,s}{1 + (\sqrt{5} + 1)t_n\,s}. \tag{5}$$

The frequency domain analysis is performed substituting the Laplace variable related to the complex frequency variable:

$$s = j2\pi f. \tag{6}$$

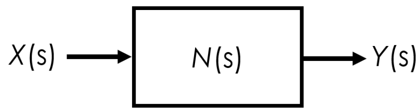

FIGURE 2. Block diagram of TF with input X and output Y.

The main parameters permitting the LP-NGD characterization are the TF magnitude $N(f) = |N(j2\pi f)|$ which is given by:

$$N(f) = \frac{\sqrt{1 + \left[2\pi(\sqrt{5} - 1)t_n f\right]^2}}{\sqrt{1 + \left[2\pi(\sqrt{5} + 1)t_n f\right]^2}}. \tag{7}$$

It should be reminded the main operation expected with the LP-NGD circuit under study is the anticipation of the signal. In other terms, to generate an output with an amplitude most similar to the input, the LP-NGD circuit should operate with unity static gain:

$$N(f \approx 0) = 1. \tag{8}$$

The GD associated to first order TF given by equation (5) is defined by:

$$GD(f) = \frac{t_n\left[(4\pi t_n f)^2 - 1\right]}{\left\{ \begin{array}{c} \left\{\left[2\pi(\sqrt{5} - 1)t_n f\right]^2 + 1\right\} \\ \left\{\left[2\pi(\sqrt{5} + 1)t_n f\right]^2 + 1\right\} \end{array} \right\}}. \tag{9}$$

The basic characteristics of LP-NGD function are established from this GD. For example, the GD value which must be a real negative value is equal to:

$$GD(f \approx 0) = t_n < 0. \tag{10}$$

According to the time-domain study of LP-NGD circuit, the NGD value represents the time-advance. This is opposite to the classical circuit where the GD is positive. The NGD cut-off frequency is the root of equation:

$$GD(f = f_n) = 0. \tag{11}$$

The following subsection examines the LP-NGD frequency domain analysis with a test case of TF from given specifications.

B. FREQUENCY DOMAIN ANALYSIS OF UNFAMILIAR LP-NGD CIRCUIT

In difference to the classical Bode diagrams, the LP-NGD analysis in the frequency domain is based on the magnitude and GD which can be calculated from equation (7) and equation (9), respectively. The general cases of magnitude and GD diagrams highlighting the NGD characterization are plotted in Figs. 3. As seen in Fig. 3(a), the magnitude response presents a gain of about 0 dB at VLFs. Fig. 3(b) explains the LP-NGD behavior of the considered TF responses.

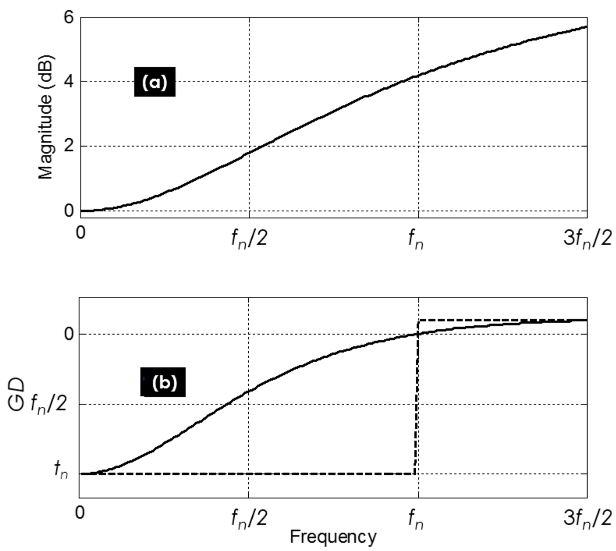

FIGURE 3. (a) Magnitude and (b) GD frequency responses of the considered LP-NGD TF.

As an illustrative application example, the LP-NGD characterization of the employed sensor and digital circuit implementation platform must be developed. Thus, the LP-NGD specification corresponding to $t_n = -30$ s time-advance is considered in the present study. Accordingly, as POC, the coefficients of LP-NGD TF introduced in equation (5) are $a = 48.5$ rad/s and $b = 18.5$ rad/s. The LP-NGD specifications from the computed results are recapitulated in Table 3.

The design formulation and analysis of digital circuits will be elaborated in the next subsection to get a larger insight into the anticipation effect on a large time scale.

C. DESIGN FORMULAS OF UNFAMILIAR LP-NGD DIGITAL CIRCUIT FOR THE SIGNAL ANTICIPATION

The LP-NGD digital circuit considered in this study is developed from the discretization of the LP-NGD canonical form defined in [25] and [26]. The main targeted specifications necessary during the synthesis are the targeted NGD value t_n which is linked to the cut-off frequency expressed in equation (3). The digital circuit corresponding to the LP-NGD TF defined by equation (5) is obtained by means of discrete instant time:

$$t = k\,T_s \tag{12}$$

knowing the sampling period T_s and incremented integer $k = \{1, 2, 3, \ldots\}$. Therefore, the discrete input and output values can be defined by:

$$\begin{cases} x[k] = x(t = k\,T_s) \\ y[k] = y(t = k\,T_s) \end{cases} \tag{13}$$

The discrete equation equivalent to the system introduced by Fig. 2 is defined by the convolution product:

$$y[k] = n[k] \otimes x[k]. \tag{14}$$

TABLE 3. Specifications of the LP-NGD function in the frequency domain.

Description	Parameter	Value
TF coefficient	a	48.5 rad/s
	b	18.5 rad/s
NGD value	$GD(f\approx0)$	-30 s
NGD cut-off frequency	$f_n(m)$	5.3 mHz
Magnitude	$N(f\approx0)$	0 dB

In function of real coefficients q_0, q_1 and q_2, the LP-NGD digital circuit can be implemented by means of difference equation:

$$y[k+1] = q_0 x[k] + q_1 x[k+1] + q_2 y[k] \tag{15}$$

by taking the initial value:

$$y[1] = x[1]. \tag{16}$$

For the case of unity static gain TF, the design formulas are expressed as:

$$q_0 = \frac{(1-\sqrt{5})t_n}{2T_s + (1+\sqrt{5})t_n} \tag{17}$$

$$q_1 = \frac{2T_s + (\sqrt{5}-1)t_n}{2T_s + (1+\sqrt{5})t_n} \tag{18}$$

$$q_2 = \frac{(1+\sqrt{5})t_n}{2T_s + (1+\sqrt{5})t_n}. \tag{19}$$

It is noteworthy that for the better integrity of the anticipated signal, the sampling and time-advance should respect the condition:

$$|t_n| \geq 4T_s. \tag{20}$$

Knowing the established innovative synthesis equations, the NGD digital circuit for anticipating sensed signals can be specifically designed. But more practical validation is needed to demonstrate if it is feasible to compute the difference equation of the unfamiliar LP-NGD digital circuit. Accordingly, a transient test with a deterministic pulse signal with a POC is conducted in the next section.

IV. ANTICIPATION RESULT OF DETERMINISTIC PULSE SIGNAL BY NGD METHOD

The unfamiliar LP-NGD digital circuit is transiently characterized by POC design in the present section. The LP-NGD digital circuit prototype is implemented on the MCU test board. The proposed characterization enables quantifying the anticipation effect with the reproducible and deterministic pulse signal. After routine algorithm exploration and computation of the LP-NGD difference equation, the obtained time-domain result is discussed.

A. LP-NGD DIGITAL CIRCUIT CODING

To start the LP-NGD digital POC design, the desired NGD specification as time-advance t_n must be defined. Then, the difference equation coefficient parameters with respect to

TABLE 4. Design coefficients of difference equation constituting the LP-NGD digital circuit POC.

Parameter	t_n	f_n	c_0	c_1	c_2
Value	-10 s	15. 9 mHz	-1.448	1.895	0.553
	-15 s	10.6 mHz	-1.702	2.052	0.65
	-20 s	7.96 mHz	-1.865	2.152	0.712
	-25 s	6.37 mHz	-1.98	2.223	0.756
	-30 s	5.3 mHz	-2.062	2.275	0.788

the STM32® MCU specifications must be calculated. From where the POC difference equation coefficient parameters were calculated via formula (17), formula (18) and formula (19). Table 4 addresses the calculated LP-NGD difference equation coefficients for different values of targeted time-advance t_n varied between -30 s and -10 s with sampling period $T_s = 5$ s. The LP-NGD POC function must be implemented from STM32 MCU active pins.

The sampled output of the LP-NGD digital circuit, expressed by difference equation (15), was computed with the recursive operation of a routine algorithm. Before the real-time temperature anticipation validation, it would be necessary to characterize the LP-NGD digital performance with deterministic signals.

The following subsection discusses the time-domain characterization experimental setup of a designed and implemented LP-NGD digital circuit with an analytical deterministic pulse signal.

B. EXPERIMENTAL SETUP OF LP-NGD DIGITAL CIRCUIT FOR DETERMINISTIC SIGNAL ANTICIPATION TEST

Fig. 4(a) introduces the MCU schematic that describes circuit details. Fig. 4(b) represents the illustrative synoptic diagram of the experimental setup. The LP-NGD circuit POC was tested by using a deterministic test signal. The input signal x is provided by the signal generator. Then, it attacks the MCU and is visualized simultaneously with the output analog voltage from pin PA5 through the DAC. As seen in Fig. 4, the MCU is powered by a USB port connected to the PC driver. During the operation test, the MCU configuration including the input and output signal interactions with the microprocessor is carried out by using the STM32CubeIDE software installed on the driver PC. The tested signal LP-NGD FIR responses are recorded in CSV format and replotted in a MATLAB® environment. The time-domain LP-NGD test is carried out with deterministic signals presenting the possibility to control specifications as bandwidth, magnitude and rise/fall fronts are needed.

Accordingly, the LP-NGD digital circuit transient characterization is discussed with deterministic pulse signal defined in the following subsection.

C. DETERMINISTIC PULSE SIGNAL DEFINITION

The test signals should have a pulse waveform to assess the input and output time-advance associated with the rising and falling edge fronts in addition to the amplitude. In addition, there is also the possibility to set the spectral bandwidth of the pulse test signal to f_n. The test signal is a symmetric pulse having a cosine waveform expressed by:

$$x(t) = x_m\left[1 - \cos\left(\frac{2\pi t}{T}\right)\right] \tag{21}$$

with average value and amplitude equal parameters to $x_{2m} = 0.5$ by means of transient plot delimited $T = 17$ minutes (min).

Based on the pulse signal test, the time-advance t_n from the transient results was assessed by equation:

$$\begin{cases} y(t) = \dfrac{x_m}{2} \\ y(t+t_n) = \dfrac{x_m}{2}. \end{cases} \tag{22}$$

The amplitude ratio from the transient results was assessed by equation:

$$\chi = \frac{\max\left[y(t)\right]}{\max\left[x(t)\right]}. \tag{23}$$

The correlation coefficients between the input and output signals are:

$$xc = xcorr\left[x(t), y(t)\right]. \tag{24}$$

To demonstrate the LP-NGD response in the time domain, an analog circuit and compare it with a digital one is simulated.

D. DISCUSSION ON THE LP-NGD TRANSIENT CHARACTERIZATION

It is worth reminding that the LP-NGD digital circuit defined by difference equation (15) was implemented in C-code as written in a routine algorithm. The time-domain results verify the forecasted ones from the frequency domain of the previous subsection. The measured and calculated real-time LP-NGD digital circuit results are depicted in Figs. 5.

Fig. 5(a) represents the transient responses of the cosine pulse. The input pulse plotted in a black solid curve by output ones from calculation plotted in a red solid curve and that one from measurement plotted in a blue dashed curve are compared. Fig. 5(b) displays the zoom into the plot showing the time-advance assessment from the leading front of input and output cosine pulses. One can understand from both results that the transient responses present a remarkable aspect of signal behavioral anticipation. Table 5 summarizes the corresponding time-domain characteristics of the LP-NGD function including the correlation coefficients between input and output signals.

As an LP-NGD digital circuit application, the following section explores the anticipation of the controlled temperature sensed by the thermistor.

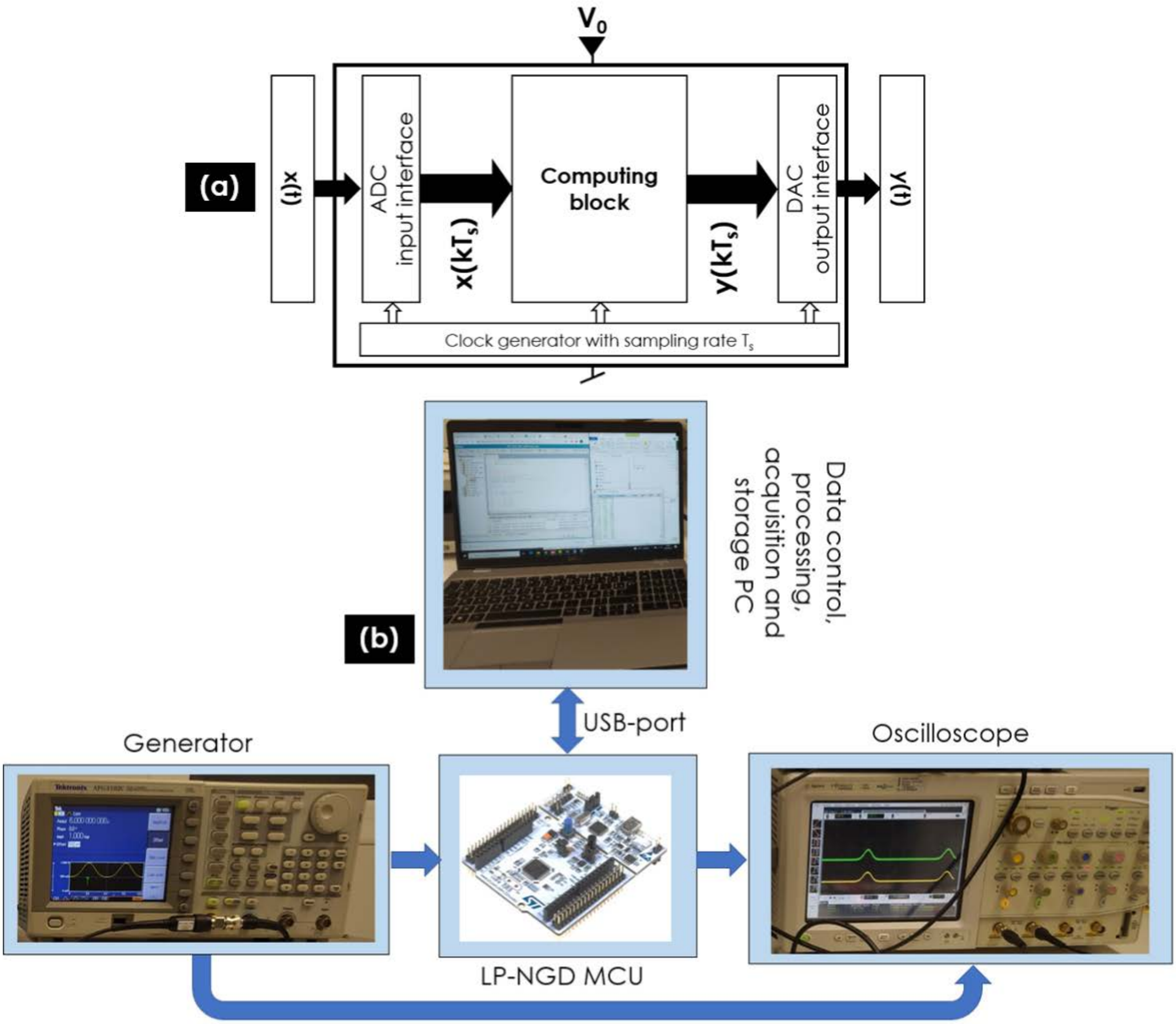

FIGURE 4. (a) Schematic of MCU and (b) synoptic diagram integrating the unfamiliar LP-NGD digital circuit experimental setup.

V. EXPERIMENTATION ANTICIPATION OF HEATED TO COOLED CYCLE TEMPERATURE VARIATION

In order to verify the feasibility of the anticipation of the temperature variation, an original demonstrator of experimentation is described in the present section. The anticipation results obtained on the thermal wave application will be discussed.

A. SPECIFICATIONS OF EMPLOYED THERMAL ROOM AND FREEZER

The technical specifications and the operation test of the thermal chamber and freezer are described in the following paragraphs.

1) EMPLOYED HEATER THERMAL ROOM SPECIFICATIONS

To heat the sensor, a commercial chamber oven is used with the possibility to control the temperature. Fig. 6 shows the photograph of the thermal chamber oven used during the test. The employed test chamber is referenced STF-N 240 [40] provided by FALC® instruments. The chamber operates with an electric heat source. It presents a capacity of 240 litres able to operate with a maximal temperature of 300°C.

The thermistor sensor is placed inside the chamber during the test. It is connected to the control PC using a USB cable. Before running the test, at the beginning of the test, the chamber temperature is equal to the ambient one, $T_a = 20$°C. Moreover, the temperature is controlled with an external monitoring command panel.

2) EMPLOYED FREEZER SPECIFICATIONS

For the freeze test, the operation is similar to the previous case of the heater. But in this case, when placed in the room, the sensor is disconnected from the driver's digital board. Fig. 7

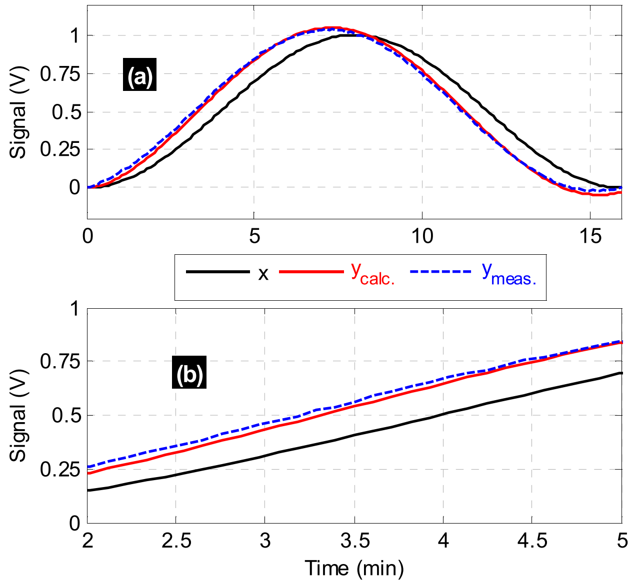

FIGURE 5. Comparison of input and calculated and measured outputs of cosine pulse in (a) wide and (b) zoomed in time window plots.

TABLE 5. LP-NGD characteristics of the implemented LP-NGD digital circuit prototype.

Approach	Input and output amplitude ratio	Time-advance	Correlation coefficient
Calculated	1.09	-1.41 min	96%
Measured	1.04	-1.46 min	98%

presents the photograph of the freezer employed to decrease the sensor temperature.

The freezer chamber is a commercial equipment referenced Candy®. The chilling test chamber presents the possibility to control the room temperature until a minimum value equal to −20°C. The freezer must be completely closed in order to reach the rapid effect of cooling on the sensor.

3) DESCRIPTION OF MCU BOARD AND TEMPERATURE SENSOR INTERCONNECTION INSIDE AND OUTSIDE THE THERMAL CHAMBER

During the developed unfamiliar LP-NGD digital circuit application experimentation, it is worth emphasizing the following test rule of thumb:

- The MCU implementation board is placed outside the oven and connected to the sensor placed in the chamber.
- The sensor to the MCU board interconnection is carried out using a long wire in order to keep the chamber closed during the test. As no current passing through, the wire length effect does not interfere with the measured temperature.
- The controlled temperature must be guaranteed uniform around the sensor. That allows changing only the temperature-sensitive element during the experiment.

The innovative experimental setup under the temperature variation cycle is summarized in the following subsection.

FIGURE 6. Picture of the thermal chamber serving for the sensor heating.

B. DESCRIPTION OF EXPERIMENTAL SETUP OF HEATED AND COOLED ARBITRARY TEMPERATURE VARIATION

One of the challenging tasks of the unfamiliar LP-NGD digital circuit application is the elaboration of the experimental protocol. The aim of the present research work is on the reproduction of industrial sensor operation environment. Fig. 8 illustrates the cycle of heated and cooled sensor experimentation. The application test of an unfamiliar LP-NGD digital circuit was carried out with respect to the cycle described by the following three phases:

- **Phase A:** At the beginning of the experimentation, the sensor is placed in the ambient temperature (of about $T_a = 25°C$) of the room of the IM2NP laboratory in Marseille.
- **Phase B:** The heating phase was performed by placing the sensor in the thermal chamber shown in Fig. 6. In this phase, the chamber temperature was increased until $T_{max} = 85°C$. The input and output of the LP-NGD circuit must be recorded and stored in the driver PC.
- **Phase C:** Then, the sensor is placed in the freezer illustrated into Fig. 7. In the present study, the temperature was decreased to −20°C.

The following subsection describes the guideline for thermal chamber operation.

C. TEST OPERATION GUIDELINE OF THE THERMAL CHAMBER

This section deals with the temperature NGD-sensored test step guideline. The test operation of the thermal chamber is summarized by the following steps:

- **Step 1:** Provide and verify the scheme of installation and connection of the temperature sensor to the input of the analog-digital converter of the microcontroller as seen in Fig. 8.
- **Step 2:** Placement of the temperature sensor in the thermal test chamber or the freezer. The sensor and the NGD digital should be interconnected by USB cable.

FIGURE 7. Picture of the employed freezer.

But the NGD digital circuit should be placed outside the chamber.

- **Step 3:** Connection of the MCU board to the PC in order to allow power supply and data transfer. The extension cable must be connected and put it into the high and low-temperature test chamber without a test circuit to ensure that the two cables entering the temperature chamber are equal in length and parallel.
- **Step 4:** In this step, the first thing to do is test the temperature measurement without a digital board. Then, the room temperature to ambient temperature T_a is adjusted. A terminal on the PC must be opened in order to retrieve, via the serial port, the predicted and measured temperature data in real-time. Then, wait for the temperature visualization.
- **Step 5:** The heating or cooling phase described in Fig. 8 must be carried out. Increase the control temperature until the expected value is stable by respecting the waiting time duration.
- **Step 6:** The previous step must be repeated by visualizing and recording the LP-NGD circuit input and output.
- **Step 7:** Data processing is a key step to end the experimentation. In this step, after the acquisition, the measured data must be downloaded. Then, the data processing should be performed by displaying program from the PC to the microcontroller.
- **Step 8:** Recovery of data in the PC terminal in order to store them in a CSV file.

The following subsection examines the results of the innovative temperature testing experimentation.

D. EXPERIMENTATION RESULT EXAMINATION SHOWING ANTICIPATION ARBITRARY TEMPERATURE VARIATION

The present subsection demonstrates the feasibility of under study NGD method anticipation with arbitrary temperature variation.

The characterization of the anticipation temperature transient results is discussed.

1) COMPARISON OF CALCULATED AND MEASURED ANTICIPATION RESULT

The original LP-NGD application test was carried out by the sensed and operating arbitrary waveform signal representing the temperature from the heater and freezer control during the real-time test. In difference to the characterization examined in subsection IV-D, in this case, the empirical investigation is based on the comparison between temperature generated by the heated and cooled sensor as input with calculated and measured LP-NGD digital circuit outputs. Figs. 9 reveal the obtained responses of chamber temperature real-time anticipation from the experimental setup displayed in Figs. 8.

Similar to the case of section IV-D, the simulated (“Calc.” plotted in the red solid line plot) and measured (“Meas.” plotted in the dotted blue plot) signals of the tested prototype of LP-NGD digital circuit are compared.

The real-time temperature test was done during $t_{max} = 43.5$ min or 2610 s with a sampling time of about $T_s = 5$ s. Once again, a good anticipation of greenhouse temperature variation is observed with good agreement between simulation and measurement.

2) SPECIFICATION ASSESSMENT OF TEMPERATURE ANTICIPATION FROM NGD METHOD

By means of the LP-NGD time-advance effect, the predicted temperature waveform is very well-correlated to the measured and sensed temperature variation. In this case, by taking $T_{ref} = 50°$C, the time-advance was assessed from the equation:

$$\begin{cases} T_{in}(t) = \dfrac{T_{ref}}{2} \\ T_{out}(t+t_n) = \dfrac{T_{ref}}{2}. \end{cases} \tag{25}$$

The amplitude ratio is assessed from local minimum and maximum of temperature T_{min} and T_{max}, in the time range from $t = 4$ min to $t = 7$ min by relation:

$$\chi = \frac{\max\left[T_{out,\max}\right]}{\max\left[T_{in,\max}\right]}. \tag{26}$$

Table 6 indicates the calculated and measured time-domain LP-NGD characteristics including the correlation coefficients between environmental and anticipated temperatures.

It can be stated that a good agreement between calculated and measured LP-NGD anticipated results.

E. STUDY OF TEMPERATURE ANTICIPATION EFFECT VERSUS TIME-ADVANCE

A test of an anticipation of the temperature is additionally investigated with respect to targeted time-advance t_n varied from -30 s to -10 s. The LP-NGD IIR equations were calculated in function of the targeted time-advances. Then,

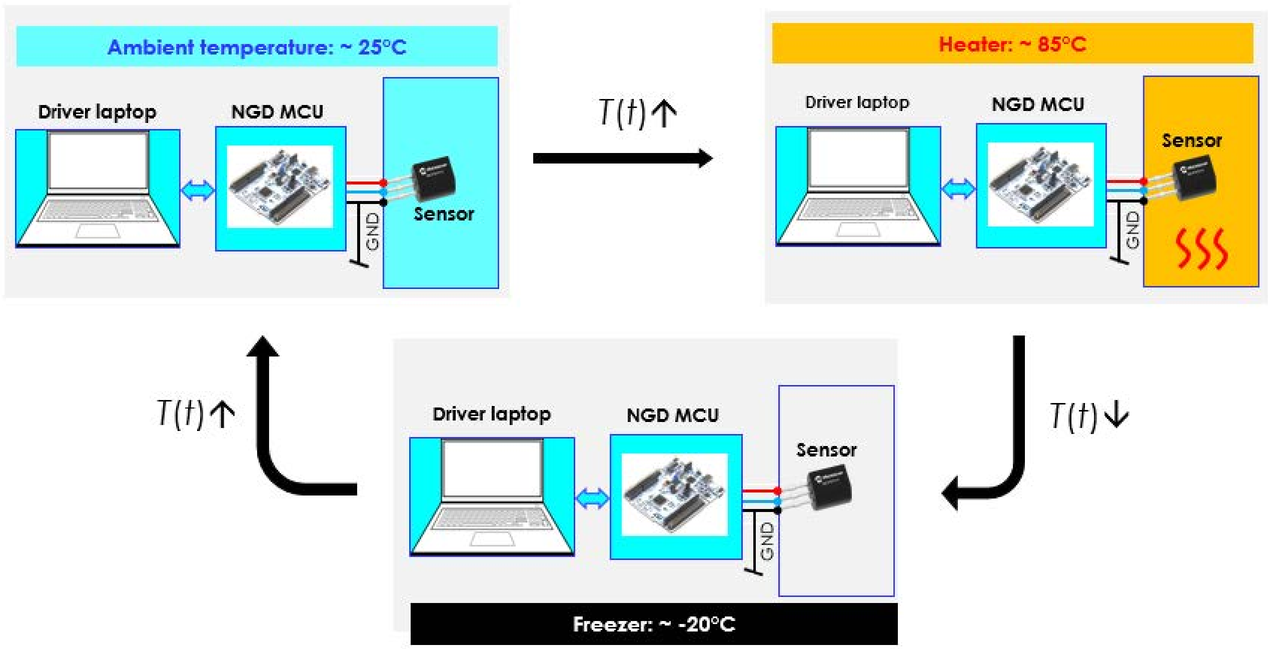

FIGURE 8. Synoptic diagram of ambient to the heated or cooled sensor experimentation.

the experimentation was performed with the same input temperature signal considered in the previous paragraph. Cartographies displayed in Fig. 10 highlight how the temperature behavior can be anticipated.

The 1-D plot of the associated transient result for the targeted different advances tn $=\{-30$ s, -25 s, -20 s, -15 s, -10 s$\}$ are shown in Fig. 11(a). It can be pointed out in the zoom observed over the time interval [4 min, 6.5 min] into the plot of fig. 11(b). The results stress once more the effectiveness of temperature anticipation linearly to the targeted time-advance. Also, it has been investigated progressively from experimentation over a varied time-advance. Once again, a notable good correlation between the environment temperature and the LP-NGD anticipated results are observed.

It can be emphasized that the anticipated temperature signal integrity is degraded with the time-advance absolute value. The cross-correlation coefficient is closer to 100% for smaller time-advance absolute value (in this case -10 s) because of the larger NGD bandwidth.

Table 7 compares the targeted and measured time-advances t_n.

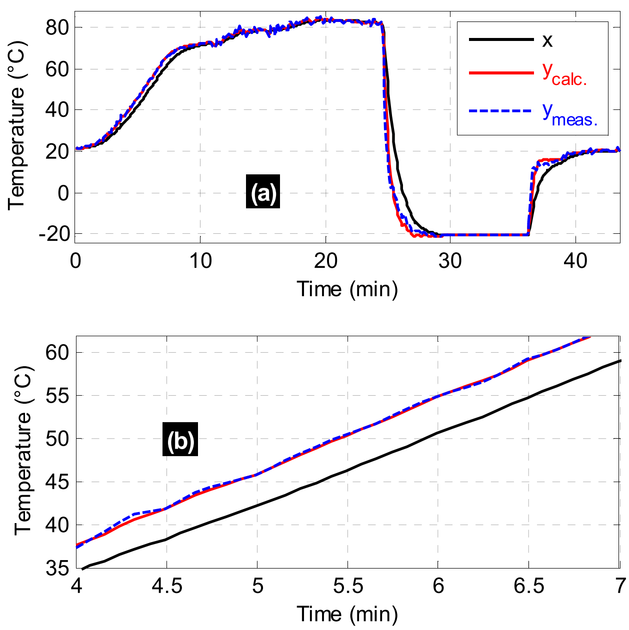

FIGURE 9. Transient results from the experimental setup shown in Fig. 8 for $t_n = -10$ s in (a) large and (b) zoomed in time window.

F. DISCUSSION ON LP-NGD DESIGN FEASIBILITY

The analysis and design method of the LP-NGD digital circuit regarding the anticipated time duration or time-advance is introduced. The unfamiliar digital circuit theory, design and implementation are described using the difference equation. A good understanding of the NGD method is explained with frequency and time domain approaches. It enables us to get insight into the signal integrity and also the NGD specifications as time-advance and cut-off frequency.

The coefficient computations of the differential equation of the designed POC with the LP-NGD digital circuit are elaborated. Two cases of the feasibility study are analysed:

- The first study case is necessary to characterize the LP-NGD circuit prototype. The test was carried out analytically by defining deterministic repeatable pulse signal. The effectiveness of the NGD method-based signal anticipation technique was confirmed by

TABLE 6. Calculated and measured LP-NGD characteristics of the implemented LP-NGD digital circuit prototype.

Approach	Input and output amplitude ratio	Time-advance	Correlation coefficient
Calculated	1.002	-0.49 min	94.1%
Measured	1.007	-0.495 min	94.7%

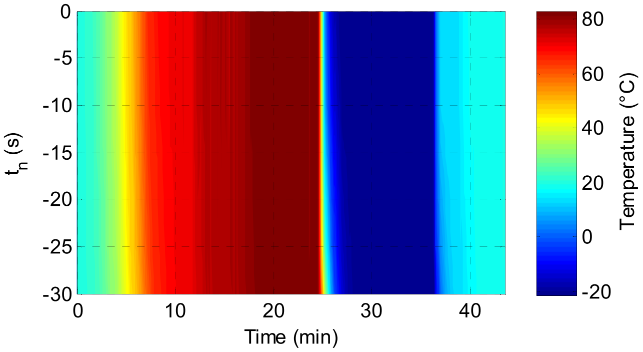

FIGURE 10. Cartography of transient result from the experimental setup shown in Fig. 8 versus pair (t_n, t).

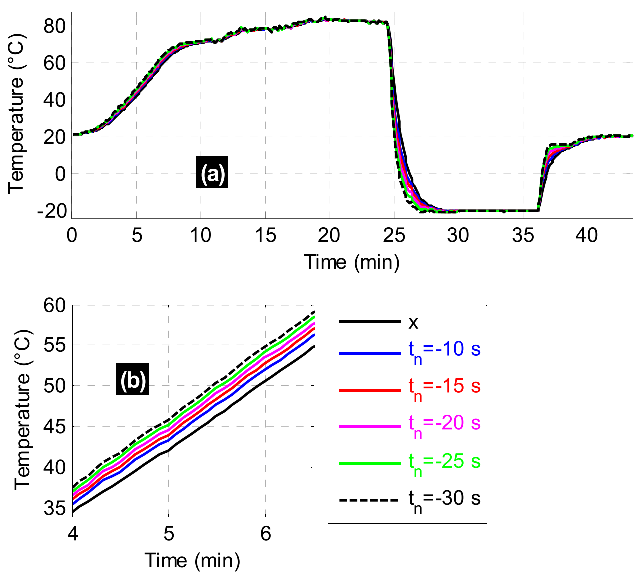

FIGURE 11. Transient results from the experimental setup shown in Fig. 8 for different targeted time-advances in (a) large and (b) zoomed in time window.

the satisfactory agreement between calculation and measurement. The LP-NGD digital circuit POC and prototype demonstrator work with minute scale time-advance. The anticipated result performance is quantitatively assessed by the time-advance and also the cross-correlation between the test pulse signal and the anticipated signal generated by the LP-NGD digital circuit.

- The second experimental work has been performed by trying to reproduce the temperature of two distinct commercial thermal chambers. The employed heater thermal chamber STF-N 240 [42] provided by FALC® instruments and freezer referenced Candy® have the

TABLE 7. LP-NGD characteristics from the results shown in Figs. 11.

Expected time-advance	Measured time-advance	Correlation coefficient
-10 s	-9.9 s	99.4%
-15 s	-14.8 s	99.1%
-20 s	-19.6 s	97.2%
-25 s	-24.5 s	95.8%
-30 s	-29.7 s	94.7%

possibility of controlling the temperature in a very wide range. The obtained results clearly demonstrate the possibility of anticipating industrial sensed signals as temperature sensors in real-time. The fascinating results show that the anticipation of the thermal wave with time-advance of the order of one minute is obtained and discussed. The assessment of the anticipation performance is defined by the time-advance of the arbitrary thermal wave signal. In addition, a very good cross-correlation is assessed between the real environment sensed and anticipated temperatures.

VI. CONCLUSION

Despite the progressive research work on NGD analog circuit design [16], [17], [18], [19], [20], [21], [22], [23], [24], [25], [26], [27], [28], [29], [30], [31], [32], [33], [34], very few studies are available on NGD digital one [35], [36]. More importantly, according to the best of the authors' knowledge, no application study on NGD digital circuits is, so far, available in the literature. Due to this scientific reason, for the first time, a pioneer work about the original application of an unfamiliar LP-NGD digital circuit for temperature variation anticipation is investigated in the present research work. The experimental investigation is innovatively performed with a completely arbitrary sensed signal in real-time. The temperature variation anticipation is empirically elaborated and experimented with using the NGD method.

An innovative test protocol of sensed temperature with a wide range of variation below 0°C and near 100°C is developed. The test configuration expected to reproduce the industrial environment is established. The experimental setup is based on the use of a commercial temperature sensor which is an active thermistor referenced MCP9701A-E/TO manufactured by Microchip® [40]. The sensor provides the thermal wave as the input signal of the LP-NGD digital circuit. The prototype of a fascinating NGD digital circuit was designed by means of a C-coded program implemented in the STM32® MCU board.

As work in progress following the present study, the authors are revolutionizing industry 4.0 technology through NGD digital circuit integration:

- Distorted signal integrity improvement with NGD equalization technique,
- Delay cancellation to improve system robustness and stability,
- And especially industrial systems and also sensors for anticipating degradation default.

REFERENCES

[1] A. Anjomshoaa, "Blending building information with smart city data," in *Proc. 5th Int. Conf. Semantics Smarter Cities*, vol. 1280, Oct. 2014, pp. 1–2.
[2] A. Thavlov and H. W. Bindner, "Thermal models for intelligent heating of buildings," in *Proc. Int. Conf. Appl. Energy (ICAE)*, Suzhou, China, Jul. 2012, pp. 5–8.
[3] L. Rajaoarisoa, M.-H. Benzaama, K. N. M'Sirdi, L. Clavier, and M. Sayed-Mouchaweh, "Switching predictive controller for building optimal thermal comfort," in *Proc. 30th Medit. Conf. Control Automat.*, Athens, Greece, Jun. 2022, pp. 127–132.
[4] L. Rajaoarisoa, B. Ravelo, W. Rahajandraibe, and L. Etienne, "Numerical weather modelling to improve energy efficiency and climate control of the buildings," in *Proc. Conf. Francophone l'Int. Building Perform. Simul. Assoc. (IBPSA)*, Reims, France, Nov. 2020, pp. 1–5.
[5] B. Ravelo, L. Rajaoarisoa, and O. Maurice, "Thermal modelling of multilayer walls for building retrofitting," *J. Building Eng.*, vol. 29, May 2020, Art. no. 101126.
[6] R. Randriatsiferana, L. Rajaoarisoa, S. Ngoho, W. Rahajandraibe, and B. Ravelo, "Zonal thermal room original model with Kron's method," *IEEE Access*, vol. 8, pp. 174893–174909, 2020.
[7] M. H. Benzaama, L. H. Rajaoarisoa, B. Ajib, and S. Lecoeuche, "A data-driven methodology to predict thermal behavior of residential buildings using piecewise linear models," *J. Building Eng.*, vol. 32, Nov. 2020, Art. no. 101523.
[8] J. M. Giachino, "Smart sensors," *Sensors Actuators*, vol. 10, nos. 3–4, pp. 239–248, Nov. 1986.
[9] P. G. Ranky, "Smart sensors," *Sensor Rev.*, vol. 22, no. 4, pp. 312–318, 2002.
[10] J.-P. Richard, "Time-delay systems: An overview of some recent advances and open problems," *Automatica*, vol. 39, no. 10, pp. 1667–1694, Oct. 2003.
[11] F. Wilches-Bernal, R. Concepcion, J. C. Neely, D. A. Schoenwald, R. H. Byrne, B. J. Pierre, and R. T. Elliott, "Effect of time delay asymmetries in power system damping control," in *Proc. IEEE Power Energy Soc. Gen. Meeting*, Chicago, IL, USA, Jul. 2017, pp. 1–5.
[12] S.-I. Niculescu, *Delay Effects on Stability: A Robust Control and Approach*, vol. 269. Berlin, Germany: Springer, 2001.
[13] M. Wu, Y. He, J.-H. She, and G.-P. Liu, "Delay-dependent criteria for robust stability of time-varying delay systems," *Automatica*, vol. 40, no. 8, pp. 1435–1439, 2004.
[14] M. Siddique, M. Rehan, M. Bhatti, and S. Ahmed, "Delay-range-dependent local adaptive and robust adaptive synchronization approaches for time-delay chaotic systems," *Nonlinear Dyn.*, vol. 88, no. 4, pp. 2671–2691, Jun. 2017.
[15] D. Solli, R. Y. Chiao, and J. M. Hickmann, "Superluminal effects and negative group delays in electronics, and their applications," *Phys. Rev. E, Stat. Phys. Plasmas Fluids Relat. Interdiscip. Top.*, vol. 66, no. 5, pp. 1–12, Nov. 2002.
[16] C. Hymel, M. Skolnick, R. Stubbers, and M. Brandt, "Temporally advanced signal detection: A review of the technology and potential applications," *IEEE Circuits Syst. Mag.*, vol. 11, no. 3, pp. 10–25, Aug. 2011.
[17] B. Ravelo, "Recovery of microwave-digital signal integrity with NGD circuits," *Photon. Optoelectron.*, vol. 2, no. 1, pp. 8–16, Jan. 2013.
[18] H. U. Voss, "Signal prediction by anticipatory relaxation dynamics," *Phys. Rev. E, Stat. Phys. Plasmas Fluids Relat. Interdiscip. Top.*, vol. 93, no. 3, pp. 1–5, Mar. 2016.
[19] M. W. Mitchell and R. Y. Chiao, "Causality and negative group delays in a simple bandpass amplifier," *Amer. J. Phys.*, vol. 66, no. 1, pp. 14–19, Jan. 1998.
[20] M. W. Mitchell and R. Y. Chiao, "Negative group delay and 'front' in a causal system: An experiment with very low frequency bandpass amplifiers," *Phys. Lett. A*, vol. 230, nos. 3–4, pp. 133–138, Jun. 1997.
[21] T. Nakanishi, K. Sugiyama, and M. Kitano, "Demonstration of negative group delays in a simple electronic circuit," *Amer. J. Phys.*, vol. 70, no. 11, pp. 1117–1121, Nov. 2002.
[22] M. Kitano, T. Nakanishi, and K. Sugiyama, "Negative group-delay and superluminal propagation: An electronic circuit approach," *IEEE J. Sel. Top. Quantum Electron.*, vol. 9, no. 1, pp. 43–51, Feb. 2003.
[23] J. N. Munday and R. H. Henderson, "Superluminal time advance of a complex audio signal," *Appl. Phys. Lett.*, vol. 85, no. 3, pp. 503–504, Jul. 2004.
[24] B. Ravelo, "Demonstration of negative signal delay with short-duration transient pulse," *Eur. Phys. J. Appl. Phys.*, vol. 55, no. 1, 2011, pp. 1–8.
[25] B. Ravelo, "Similitude between the NGD function and filter gain behaviours," *Int. J. Circuit Theory Appl.*, vol. 42, no. 10, pp. 1016–1032, Oct. 2014.
[26] B. Ravelo, "First-order low-pass negative group delay passive topology," *Electron. Lett.*, vol. 52, no. 2, pp. 124–126, Jan. 2016.
[27] B. Ravelo, "Baseband NGD circuit with RF amplifier," *Electron. Lett.*, vol. 47, no. 13, pp. 752–754, Jun. 2011.
[28] B. Ravelo, "Methodology of elementary negative group delay active topologies identification," *IET Circuits Devices Syst.*, vol. 7, no. 3, pp. 105–113, May 2013.
[29] B. Ravelo, "Theory on negative time-delay looped system," *IET Circuits, Devices Syst.*, vol. 12, no. 2, pp. 175–181, Mar. 2018.
[30] B. Ravelo, "Negative group-delay phenomenon analysis with distributed parallel interconnect line," *IEEE Trans. Electromagn. Compat.*, vol. 58, no. 2, pp. 573–580, Apr. 2016.
[31] B. Ravelo, "Theory on coupled line coupler-based negative group delay microwave circuit," *IEEE Trans. Microw. Theory Techniques*, vol. 64, no. 11, pp. 3604–3611, Nov. 2016.
[32] B. Ravelo, "Innovative theory on multiband NGD topology based on feedback-loop power combiner," *IEEE Trans. Circuits Syst. II, Exp. Briefs*, vol. 63, no. 8, pp. 738–742, Aug. 2016.
[33] B. Ravelo, "Elementary NGD IIR/FIR systems," *Int. J. Signal Process. Syst.*, vol. 2, no. 2, pp. 132–138, Dec. 2014.
[34] B. Ravelo, M. Guerin, W. Rahajandraibe, V. Gies, L. Rajaoarisoa, and S. Lallechere, "Low-pass NGD numerical function and STM32 MCU emulation test," *IEEE Trans. Ind. Electron.*, vol. 69, no. 8, pp. 8346–8355, Aug. 2022.
[35] B. Ravelo, M. Guerin, W. Rahajandraibe, and L. Rajaoarisoa, "All-pass NGD FIR original study for sensor failure detection application," *IEEE Trans. Ind. Electron.*, early access, Oct. 18, 2022, doi: 10.1109/TIE.2022.3213904.
[36] A. Maiti, A. A. Kist, and A. D. Maxwell, "Real-time remote access laboratory with distributed and modular design," *IEEE Trans. Ind. Electron.*, vol. 62, no. 6, pp. 3607–3618, Jun. 2015.
[37] P.-Y. Chen, S. Yang, and J. A. McCann, "Distributed real-time anomaly detection in networked industrial sensing systems," *IEEE Trans. Ind. Electron.*, vol. 62, no. 6, pp. 3832–3842, Jun. 2015.
[38] *Low-Power Linear Active Thermistor ICs*, Standard MCP9700/9700A and MCP9701/9701A, Microchip, Chandler, AZ, USA, Jun. 2022, pp. 1–22.
[39] *Datasheet-Production Data*, Standard STM32L476xx, ST, Jun. 2019.
[40] *Chamber Oven STF-N 240*. Accessed: Jun. 10, 2022. [Online]. Available: https://www.directindustry.fr/prod/falc-instruments-srl/product-106753-1852056.html

BLAISE RAVELO (Member, IEEE) is currently a University Full Professor at NUIST, Nanjing, China. He is also a Lecturer of circuit and system theory, STEM (science, technology, engineering, and maths), and applied physics. He is a Pioneer of the Negative Group Delay (NGD) concept, theory, design, fabrication, test, and applications. This extraordinary concept is potentially useful for anticipating and prediction all kind of information. He was the Research Director of 11 Ph.D. students (ten defended), postdocs, research engineers, and master's internships at USA, Chinese, Indian, European, and African partners. He is actively involved and contributes on several international research projects. He is the coauthor of more than 380 scientific research papers in new technologies published in international conference and journals. His research interests include multiphysics and electronics engineering. He is a member of *IET Electronics Letters*, Scientific Technical Committee of Advanced Electromagnetic Symposium (AES), and a research groups: URSI, GDR Ondes, and Radio Society. He is also the Editorial Board as *Circuit and System* Subject Editor. He is ranked in Top two world's scientists based on years from 2020 to 2022 by Stanford University, USA. He regularly invited to review papers submitted for publication to international journals IEEE TRANSACTIONS ON MICROWAVE THEORY AND TECHNIQUES, IEEE TRANSACTIONS ON CIRCUITS AND SYSTEMS, IEEE TRANSACTIONS ON ELECTROMAGNETIC COMPATIBILITY, IEEE TRANSACTIONS ON INDUSTRIAL ELECTRONICS, IEEE ACCESS, IET CDS, and IET MAP), and books (Wiley and Intech Science). He has a Google Scholar H-index is 27 and i10-index is 84.

MATHIEU GUERIN (Member, IEEE) received the Engineering degree in microelectronics and telecommunications from Polytech Marseille, in 2010, and the research master's degree in integrated circuits design and the doctorate degree from the University of Aix-Marseille, in 2010. He worked as a Technical Leader of the Analog and Radio-Frequency Design Team, IDEMIA-StarChip, for five years and designed chips embedded in SIM cards and contactless bank cards with biometric recognition. He joined Aix-Marseille University, as an Assistant Professor, in 2020, and joined CCSI Team of the IM2NP Laboratory. He is also working on methods of modeling and characterizing circuits in analog electronics. His research interest includes design and synthesis of circuits in digital electronics.

JAROSLAV FRNDA (Senior Member, IEEE) was born in Slovakia, in 1989. He received the M.Sc. and Ph.D. degrees from the Department of Telecommunications, VSB–Technical University of Ostrava, Czechia, in 2013 and 2018, respectively. He is currently working as an Assistant Professor at the University of Zilina, Slovakia. He has authored and coauthored more than 50 journal articles in Web of Science. His research interests include quality of multimedia services in IP networks, data analysis, and machine learning algorithms.

LALA RAJAOARISOA (Member, IEEE) received the M.Sc. and Ph.D. degrees in automatic and computer sciences from the University of Aix-Marseille, France, in 2005 and 2009, respectively. He is currently an Assistant Professor with the Institut Mines-Télécom Nord Europe. He is involved in research activities dedicated to the optimization of energy efficiency of smart building systems and the control and management of intelligent hydraulic systems, with more than 80 papers published in refereed journals and conferences. He regularly participates and contributes to several international and French national projects (ANR, FUI, Chist-Era, and INTERREG) and the supervisor of more than 15 Ph.D. students, postdocs, research engineers, and master's internships. This development includes the analysis of intrinsic properties such as stability, observability, identifiability, and controllability. His research interests include development of data-driven tools and methods for the observation, control of large-scale distributed systems, develop predictive models, and controllers to assess system behavior and optimize its performance.

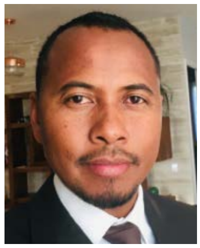

WENCESLAS RAHAJANDRAIBE (Member, IEEE) received the B.Sc. degree in electrical engineering from Nice Sophia-Antipolis University, France, in 1996, the M.Sc. degree (Hons.) in electrical engineering from the Department of Science, University of Montpellier, in 1998, and the Ph.D. degree in microelectronics from the University of Montpellier. He is currently a Full professor at the University of Aix-Marseille. In 1998, he joined the Microelectronics Department of Informatics, Robotics and Microelectronics Laboratory of Montpellier (LIRMM). In 2003, he joined the Microelectronic Department of Materials, Microelectronics, and Nanoscience Laboratory of Provence (IM2NP), Marseille, France, where he was an Associate Professor. Since 2014, he has been a Professor at Aix Marseille University, where he heads the Integrated Circuit Design Group, IM2NP Laboratory. He is regularly involved to participate and to lead the National and International Research Projects (ANR, H2020, and FP7 KIC-InnoEnergy). He has directed and co-supervised 18 Ph.D. and 15 master's students. He is the author or coauthor of 11 patents and more than 150 papers published in refereed journals and conferences. His research interests involve AMS and RF circuit design from transistor to architectural level. His current research activity is focused on ultralow power circuit design for smart sensor interface and embedded electronic in bioelectronic and e-health applications, wireless systems, design technique, and architecture for multi-standard transceiver. He is an expert of the ANR and the French Agency of Research. He has served on program committees for IEEE, NEWCAS, and ICECS. He has been and is a Reviewer of contributions submitted to several IEEE conferences and journals, such as ISCAS, NEWCAS, MWSCAS, ESSCIRC, ESSDERC, RFIC, IEEE Transactions on Circuits and Systems—I: Regular Papers, IEEE Transactions on Circuits and Systems—II: Express Briefs, *IET Electronics Letters*.